Simulating the early mpox outbreak: Dynamic-spread assessment via vSEIR model and kink detection in disease transmission*

Jian Zhou[a], Rui Xu[b], Haoran Gu[b], Junyang Cai[a,*]

[a]*School of Management, Shanghai University, Shanghai 200444, China*
[b]*School of Science, Shanghai University, Shanghai 200444, China*

Abstract

This paper proposes a varying coefficient Susceptible-Exposed-Infected-Removed (vSEIR) model to dynamically simulate the early mpox epidemic that sparked panic in 2022, considering the time-varying infection rate and the group protected by the smallpox vaccination. We apply the recursive least squares algorithm with a forgetting factor for real-time identification of time-varying infection rates and the efficacy of non-pharmacological interventions. The sparse Hodrick-Prescott (HP) filter, tuned with leave-one-out cross-validation, captures mpox epidemic kinks via the effective reproduction number R_t obtained from the discrete vSEIR model. We experiment with this approach in Brazil, Spain, UK and US, comparing COVID-19 and mpox outbreaks based on those kinks and transmission cycles, identifying that except for Spain, mpox epidemic reached its decline period earlier than COVID-19 without strong interventions. Additionally, the result regarding sensitivity analyses shows that the total number of mpox outbreak infections would have increased by 12% without smallpox vaccination and the data uncertainty can bring great variations in R_t.

Keywords: Mpox, vSEIR model, Recursive least squares algorithm, Effective reproduction number, Sparse HP filter, Sensitivity analysis

1. Introduction

1.1. Motivation and incitement

In 2022, mpox[1] had garnered significant attention due to the tens of thousands of infections it has caused worldwide, particularly in Europe and the southern US[2] [1]. On July 23, 2022, WHO declared this outbreak a public health emergency of international concern, which can cause patients with rashes and fever.

When encountering a relatively new infectious disease outbreak, governments are often caught off guard and cannot implement effective prevention and control measures due to the little knowledge regarding the epi-

*The data and sample code related to this paper are openly available at `https://github.com/masterspark2/vSEIR-monkeypox-modelling`.

*Corresponding author
Email address: `cjy0502@shu.edu.cn` (Junyang Cai)

[1]The World Health Organization (WHO) announced *mpox* as the new name for *monkeypox* on November 28, 2022 to avoid possible stigma caused by the original name.

[2]`https://www.who.int/emergencies/disease-outbreak-news/item/2022-DON385` (retrieved on 25th February 2023)

demic. Several studies have examined the monkeypox virus and its pathophysiology, as well as the histopathological data [2, 3, 4]. These findings highlight the urgent need for the development of effective therapeutics to prevent the potential rebound mpox. However, because no strict control measures have been introduced in the early outbreaks, the transmission speed of the epidemic will vary greatly every day, so the mathematical models with fixed parameters often provide relatively little information regarding the transmission cycle and the current situations during the outbreak. Hence, it is of tremendous significance to develop a rational mathematical model capable of dynamically simulating the transmission of mpox during its initial outbreak.

1.2. Literature review

In the wake of the COVID-19 pandemic, the use of infectious disease modelling with time-varying coefficients has garnered increasing attention in pandemic modelling research. These models are able to dynamically reflect the effectiveness of non-pharmacological interventions such as government strategies or public awareness of social distancing measures, allowing for more accurate simulation of epidemic situations in different countries. A number of studies have applied these models to the COVID-19 pandemic, including Yan et al. [5], who proposed a locally weighted kernel regression estimator for estimating time-varying coefficients in the varying coefficient susceptible-infected-asymptomatic-diagnosed-removed (vSIADR) model and successfully simulated epidemic situations in 25 countries. Song et al. [6] developed an extended Kalman filter for estimating and predicting the dynamic spread of COVID-19 in US and China using a maximum likelihood estimation method for online estimation of time-varying model parameters. Cai and Zhou [7] proposed a two-stage approach for estimating time-varying coefficients with their varying coefficient susceptible–infected–removed–susceptible (vSIRS) model, which they used to identify the role of unconfirmed asymptomatic infected individuals in driving the COVID-19 pandemic in US. These studies demonstrate the value of infectious disease modelling with time-varying coefficients in understanding and predicting the spread of infectious diseases such as COVID-19 as well as the role of vaccination in controlling an epidemic.

Although various pandemic modelling articles have delved into the transmission mechanism of COVID-19, there are few models that can be directly applied into mpox dynamic modelling for their over-refined compartment structure, which hinders our understanding of its potential future spread and transmission cycle. Additionally, the existing monkeypox modelling uses fixed parameters and there is no consideration of protection from smallpox vaccine [8], which is a feature of mpox epidemic. For example, Zhang et al. [9] used a modified SEIR model developed for COVID-19 to forecast and simulate mpox transmission and vaccination scenarios. The results of these predictions, however, may not be reliable since the virological relationship between SARS-CoV-2 and mpox is not exactly the same. Olumuyiwa et al. [10] developed a fractional order mathematical model to simulate mpox transmission dynamics. Nonetheless, the high dimensionality of this model makes it difficult to apply to research in various countries or other diseases. Olumuyiwa et al. [11] had also proposed a deterministic compartmental model with a relatively low dimension, but the model coefficients were fixed and some of the remaining coefficients were assumed, which reduces the applicability of the model to the mpox outbreak.

In conclusion, the current modelling approach for mpox fails to accurately and dynamically represent the characteristics of mpox outbreaks. Its reliance on fixed and assumed coefficients limits its applicability to early outbreaks in various locations. A more effective model, therefore, would take into account smallpox vaccine immunity and time-varying coefficients to accurately reflect the mpox outbreak.

1.3. Innovative contributions

Our first contribution is that we established a varying coefficient Susceptible-Exposed-Infected-Removed (vSEIR) model according to the characteristics of mpox transmission and the proportion of population age in each country for their different resistance to mpox[3] [12]. Through our model, the mpox outbreak can be accurately and dynamically simulated, addressing the limitations of existing models.

Secondly, in terms of coefficient estimation, to the best of our knowledge, we are the first to introduce the recursive least squares algorithm with a forgetting factor (FRLS), which is extensively utilized in signal adaptive filtering analysis [13], into the online estimation of the time-varying infection rate, dynamically reflecting the non-pharmacological interventions of various countries and the change in public awareness of mpox prevention.

On top of that, there is an extremely dearth of research specifically addressing the kinks and transmission period of mpox outbreak. In order to explore the transmission cycle of mpox, we consider using the sparse Hodrick-Prescott (HP) filter to produce piecewise estimators of the effective reproduction number. This method allows us to capture the kinks in the mpox in an objective and explainable way. The framework of methodology related to our paper is shown in Fig. 1, which will be further explained in the following section. Through this framework, we capture the kinks of the mpox via filtered effective reproduction numbers and conclude the periods of mpox in those four countries.

1.4. Organization of the paper

The remaining paper is structured as follows. In Section 2, we build up the vSEIR model as well as estimate the coefficient using FRLS. After that, in Section 3, the sparse HP filter is utilized to produce the piecewise estimation of the effective reproduction number of mpox and COVID-19. Next, we conclude the simulation result and compare the effective reproduction number with COVID-19 in Section 4. We also capture the kinks as well as define the periods of those two viruses in the four countries. In Section 5, two sensitivity analyses of our model are made and we provide comprehensive insights for different situations. Eventually, we summarize our results, contributions, and provide concluding discussions in Section 6.

[3] `https://www.who.int/emergencies/disease-outbreak-news/item/2022-DON396` (retrieved on 25th February 2023)

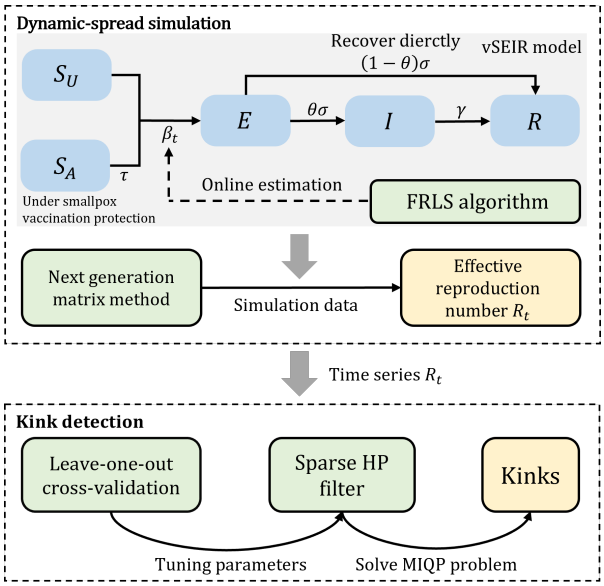

Figure 1: Framework of methodology in our paper.

2. vSEIR model

Based on the literature review in Section 1.2, we find that the existing mpox simulation models lack accuracy and fail to dynamically represent the initial outbreak. By using a time-varying coefficient, our model can dynamically monitor the strength of non-pharmacological interventions and provide a more accurate representation of the spread of the disease in various countries. This approach allows our model to compensate for the shortcomings of previous models and provide more accurate and comprehensive insights into the mpox epidemic.

In this section, we describe the details of our model and calculate the effective reproduction number as well as estimate the time-varying infection rate with FRLS algorithm. We begin by presenting the formula of the vSEIR model and the conditions that make it suitable for modelling the mpox epidemic and calculate the effective reproduction number in Section 2.1. Last we introduce the FRLS algorithm and use this algorithm in the online estimation of the time-varying infection rate in Section 2.2.

2.1. Model formulation

The vSEIR model could be divided into the following compartments according to individuals' properties as unaged susceptible compartment S_U, aged susceptible compartment S_A, exposed compartment E, infected compartment with symptoms of rashes I and removed compartment R, where σ and γ denote the incubation and recovery rate. Compartment S_A denotes a less probably-infected group of susceptible people, which has the probability of τ to encounter the infection of mpox because of the vaccination of smallpox for its 90% genomic homology with the smallpox virus. [14, 15, 16]. The removed compartment R in mpox modelling represents only the recovered individuals, neglecting the death compartment because the number of deaths in mpox epidemic is relatively small. For example, up to September 30, 2022, there were only 2 reported deaths

in US. Since we define the compartment I as infected people with rash symptoms for that mpox infections are mainly caused by skin contact, the $(1-\theta)$ proportion of the individual number in E will be transformed into compartment R directly, where θ denotes the proportion of rash symptoms among the infected group. In other words, since we define the infected compartment I as individuals with rash symptoms, then a proportion of $(1-\theta)$ from compartment E will be directly transferred to compartment R due to the lack of rash symptoms[4].

Through the definition of our model, the total population N is given by

$$N = S_A(t) + S_U(t) + E(t) + I(t) + R(t)$$

and the total number of the reported confirmed cases is given by $C(t) = I(t)+R(t)$, where $S_A(t), S_U(t), E(t)$, $I(t), R(t)$ are the numbers of individuals of each compartment in day t. Overall, the discrete structure of the proposed vSEIR model is presented in Fig. 1 and can be expressed as

$$\begin{cases} S_A(t+1) = S_A(t) - \dfrac{\beta_t \tau S_A(t) I(t)}{N} & \text{(1a)} \\ S_U(t+1) = S_U(t) - \dfrac{\beta_t S_U(t) I(t)}{N} & \text{(1b)} \\ E(t+1) = E(t) + \dfrac{\beta_t S_U(t) I(t)}{N} + \dfrac{\beta_t \tau S_A(t) I(t)}{N} - \sigma E(t) & \text{(1c)} \\ I(t+1) = I(t) + \theta\sigma E(t) - \gamma I(t) & \text{(1d)} \\ R(t+1) = R(t) + \gamma I(t) + (1-\theta)\sigma E(t). & \text{(1e)} \end{cases}$$

In particular, β_t is the time-varying infection rate. The time-varying infection rate in the model reflects the changing aspects of the mpox pandemic in terms of transmission processes and government policies designed to control the spread of the disease. The infection rate also reflects the varying effectiveness of public awareness campaigns and changes in individual behavior, such as social distancing and blistering the skin.

In addition, an extremely essential index evaluating the seriousness of an epidemic in disease modelling is the effective reproduction number R_t. It represents the average number of potential secondary cases that could be infected by an infected individual at a specific time t. Knowing the effective reproduction number during an epidemic outbreak is vital in policy making because the R_t value will indicate the current situation of an epidemic and, if the value of R_t is below 1, it means the actively infected people may be on the decline. Therefore, analyzing the R_t value can help governments make informed decisions. We conduct the R_t estimation using the next generation method [17], the corresponding derivation process is listed in Appendix A and we can obtain

$$R_t = \frac{\theta}{\gamma} \frac{(\tau\beta_t S_A(t) + \beta_t S_U(t))}{N}. \quad (2)$$

[4] `https://www.cdc.gov/poxvirus/monkeypox/cases-data/technical-report.html` (retrieved on 25th February 2023)

2.2. Estimation of time-varying parameters

In this section, we mainly focus on estimating the time-varying coefficient β_t. First, we build the base equation by adding the last three equations in difference form of vSEIR model (1), then we can get

$$E(t+1) + I(t+1) + R(t+1) = \frac{(\tau S_A(t)I(t) + S_U(t)I(t))\beta_t}{N} + E(t) + I(t) + R(t). \tag{3}$$

Furthermore, by considering the daily increments of $I(t)$, $R(t)$, and $E(t)$ in the difference form of the vSEIR model (1), denoted as $\Delta I(t+1) = I(t+1) - I(t)$, $\Delta R(t+1) = R(t+1) - R(t)$, and $\Delta E(t+1) = E(t+1) - E(t)$, Eq. (3) can be further induced as

$$\Delta E(t+1) + \Delta I(t+1) + \Delta R(t+1) = \frac{(\tau S_A(t)I(t) + S_U(t)I(t))\beta_t}{N}. \tag{4}$$

Notice that the value of $E(t)$ cannot be obtained directly while the value of $\Delta I(t+1) + \Delta R(t+1)$ is equal to the daily increment of the confirmed cases, that is,

$$\Delta C(t+1) = C(t+1) - C(t) = \Delta I(t+1) + \Delta R(t+1)$$

. Then to get the value of $E(t)$, the following substitution can be made by $\Delta C(t) = \sigma E(t)$. By the substitution of $\Delta C(t)$, the estimation of $E(t)$ can be further expressed as

$$E(t) = \frac{\Delta C(t)}{\sigma}. \tag{5}$$

Next, we start to estimate the time-varying infection rate with the FRLS algorithm. The FRLS algorithm uses the principle of the least squared error to solve the optimal model parameters in the field of engineering and bioinformatics, such as signal processing [18] and filter coefficients updating [19]. The main feature of FRLS is that it has a flexible update frequency and can provide a great simulation outcome, which can effectively reflect the transmission characteristics of the outbreak period. Moreover, compared with the work of Yan et al. [5], the FRLS algorithm is based on past and current data to update the time-varying parameters. This is superior to the locally weighted kernel regression estimator, which requires past and future information and can result in future information leakage, making the model unexplainable. Besides, deep learning techniques are also utilized to estimate the time-varying infection rate [20, 21]. However, when confronted with limited epidemic data, neural networks that rely on a substantial volume of input data frequently fail to generate results of higher reliability. On the contrary, the FRLS algorithm depends less on the scale of data, which is more suitable for the estimation of epidemic parameters during the outbreak. Therefore, the FRLS algorithm makes our model more reliable in estimating the time-varying infection rate because the FRLS updates the vital transformation on a daily basis and the use of forgetting factor gives the later data more abilities to influence the simulation model, which is reasonable in the spread of the epidemic. Since this is a dynamic model with time-varying coefficients, it will be easier to detect the strength of non-pharmacological interventions.

Specifically, let

$$X_t = \frac{\tau S_A(t)I(t) + S_U(t)I(t)}{N} \tag{6}$$

and

$$Y_t = \Delta E(t+1) + \Delta I(t+1) + \Delta R(t+1). \tag{7}$$

We regress Y_t on X_t by the FRLS algorithm, which builds the bridge between β_{t-1} and β_t. The main process could be followed by those several steps. First, denote the medium value as

$$P_t = \frac{1}{X_t^2}$$

and the gain value as

$$k_t = \frac{P_{t-1}X_t}{\lambda + X_t^2 P_{t-1}}, \tag{8}$$

where λ is a forgetting factor, which is introduced because we consider the later data to be of greater importance. When λ is closer to 1, the algorithm does not cast much weight on the updated data. On the contrary, the algorithm prefers the updated data more when λ is closer to 0. Then to update β_t, we first update P_t by

$$P_t = \frac{1}{\lambda}P_{t-1} - \frac{1}{\lambda}k_t X_t P_{t-1}. \tag{9}$$

Finally, we update the infection rates for the transformation from S_A, S_U to E by

$$\beta_t = \beta_{t-1} - k_t \left(X_t \beta_{t-1} - Y_t\right). \tag{10}$$

Overall, the whole estimation process via FRLS could be conducted in Algorithm 1 in Appendix B. After estimating β_t, we can get the value of the vSEIR model and the effective reproduction number on a daily basis.

3. Finding kinks in mpox epidemic

Kinks of a biological process refer to the points that change the upward or downward direction of the curve, intuitively speaking, the kinks are the points where the tangent crosses the curve [22]. In an epidemic, the kinks often indicate the change of infection speed, affecting the health policy, disease control programs, and even the daily life of the public. During the COVID-19 epidemic, finding the kinks of the pandemic is of great importance because it can inform the public about the future situation of the epidemic and inform the government about future policies.

In this section, we use the sparse Hodrick-Prescott (HP) filter to capture the kinks of mpox epidemic and identify its transmission cycle. The sparse HP filter that can be utilized to capture kinks in the filtered effective reproduction number is introduced in Section 3.1. The sparse HP filter above allows us to objectively and explainably represent those kinks, providing insight into the epidemic situation and the spread of the mpox virus. In Section 3.2, we describe the method used to select the optimal tuning parameters for the sparse HP filter.

3.1. Sparse Hodrick-Prescott filter

We use the sparse HP filter that adds a constraint onto the original HP filter [23]. The constraint ensures that the filtered value of R_t is piecewise smooth except for the kinks. We believe that using kinks, which are obtained through a mathematical filtering method, is more objective and explainable than using sharp changes in the R_t curve or certain dates of government issues in defining epidemic periods. By using periods based on these kinks, we can more accurately explain the transmission cycle in our model. In our model, we define the kinks as Definition 1, which differs from Lee et al.'s definition for a better representation of the outbreak situation [23].

Definition 1 (Kinks). *The set of kinks in the filtered effective reproduction number series r_t is defined by $\{t \mid r_t - r_{t-1} \neq r_{t+1} - r_t$ for $t = 1, 2, \ldots, T-1\}$, where T is the length of the experiment period.*

We use a sparse version of the HP filter [23], which is

$$\begin{cases} \min \ \sum_{t=0}^{T} \left(R_t - r_t\right)^2 + \mu \sum_{t=1}^{T-1} \left(r_{t-1} - 2r_t + r_{t+1}\right)^2 \\ \text{subject to:} \\ \quad \sum_{t=1}^{T-1} \mathbf{1}\left\{r_t - r_{t-1} \neq r_{t+1} - r_t\right\} \leq \chi, \end{cases} \tag{11}$$

where $\mathbf{1}\{\cdot\}$ is an indicative function, if the $\{\cdot\}$ is true, then $\mathbf{1}\{\cdot\}$ is 1, otherwise 0. The constraint in programming problem (11) controls how many kinks are allowed. To simplify the calculation, the programming problem (11) can be changed into a mixed-integer quadratic programming (MIQP) problem as

$$\begin{cases} \min \ \sum_{t=0}^{T} \left(R_t - r_t\right)^2 + \mu \sum_{t=1}^{T-1} \left(r_{t-1} - 2r_t + r_{t+1}\right)^2 \\ \text{subject to:} \\ \quad \sum_{t=1}^{T-1} z_t \leq \chi \\ \quad -Mz_t \leq r_{t-1} - 2r_t + r_{t+1} \leq Mz_t, \ t = 1, 2, \ldots, T-1 \\ \quad \min_{t=0,\ldots,T} \{R_t\} \leq r_t \leq \max_{t=0,\ldots,T} \{R_t\} \\ \quad M = \max_{t=1,\ldots,T-1} \{R_{t-1} - 2R_t + R_{t+1}\} \\ \quad z_t \in \{0, 1\}, \ t = 1, 2, \ldots, T-1, \end{cases} \tag{12}$$

where r_t is the decision variable being filtered, and z_t is the auxiliary variable that represents the kink, that is, t is the kink if $z_t = 1$. The MIQP problem (12) can be solved via a branch and bound algorithm, which consists of a systematic enumeration of candidate solutions by means of state space search [24]. Specifically, we can solve this problem via a state-of-the-art commercial mathematical programming solver, e.g., Gurobi with python API. The kinks of mpox can thus be found through the filtered R_t values.

3.2. Selection of tuning parameters in mpox simulation

There are two tuning parameters in our sparse HP filter, μ and χ. For each pair of (χ, μ), let $\hat{r}_{-s}(\chi, \mu)$ denote the leave-one-out filtered value of original R_t. The leave-one-out cross-validation can produce a result closest to the expected value of training the entire test set, which is widely used in machine learning and recently, it has been applied to epidemic modelling to find optimal parameters [5]. To be more concrete, for each pair of (χ, μ), we filter the original R_t by whole data except for the day s, that is, we change the objective function in programming problem (11) into

$$\min \sum_{t=0, t\neq s}^{T} \left(R_t - r_t\right)^2 + \mu \sum_{t=1}^{T-1} \left(r_{t-1} - 2r_t + r_{t+1}\right)^2 .$$

Therefore, we choose the optimal (χ, μ) by

$$\min_{(\chi,\mu)\in X\times U} \sum_{t=0}^{T} \left(R_t - \hat{r}_{-t}(\chi, \mu)\right)^2 , \tag{13}$$

where X and U denote the possible sets of χ and μ. In the next section, we will do the tuning parameters selection based on criterion (13).

4. Experimental results of the vSEIR model and the sparse HP filter

We select four main countries with the extensive spread of the mpox virus, in concrete, Brazil, Spain, UK, and US. The earliest case among them is May 06, 2022, UK. Then we calculate the simulation of mpox cases as well as the effective reproduction number of the mpox and COVID-19, and then we make a comparison between them on R_t. The model we use in the COVID-19 simulation is similar to the vSEIR model used in the mpox simulation, which is listed in Appendix C. To get insights about the transmission cycle, we utilize the sparse HP filter to produce the piecewise estimator of effective reproduction number and find the kinks of the mpox and COVID-19 epidemic, a comparison and analysis are conducted based on those kinks. Finally, we make an analysis of the surveillance and policy implications by measuring effective reproduction number growth rates.

4.1. Data

The population data are available on Wikipedia and the time series of confirmed cases are accessible on GitHub[5] [25]. We use the Moving Average method to conduct data smoothing. Table 1 shows the basic data and initial values of S_A and S_U of the four main countries of mpox infection. The initial value of the exposed compartment E is 8 times the number of the infected compartment I according to the incubation period. The vaccine failure rate is based on WHO, which states that people who got vaccinated against smallpox have nearly 15% of the chances to be infected[6] and the boundary for S_A and S_U is 55 based on the year of

[5] `https://github.com/globaldothealth/monkeypox` (retrieved on 27th February 2023)

[6] `https://www.who.int/news-room/fact-sheets/detail/monkeypox` (retrieved on 28th February 2023)

Table 1: The mpox data of the four countries being estimated

Country	Date Range	N	$S_A(0)$	$S_U(0)$	$I(0)$
UK	2022.05.06 $\sim$ 2022.09.25	67,220,000	17,477,143	49,742,640	24
US	2022.05.17 $\sim$ 2022.09.25	332,854,719	79,885,065	252,969,373	35
Spain	2022.05.18 $\sim$ 2022.09.25	47,350,392	14,678,548	32,671,609	26
Brazil	2022.06.08 $\sim$ 2022.09.25	212,600,000	31,889,962	180,709,785	28

last batch of uniformly vaccinated against smallpox. For the time from exposure to rash onset, we estimated a mean incubation period of 8.7 days (95% confidence interval: 6.9 $\sim$ 11.7) with a standard deviation of 1.6 days (95% confidence interval: 1.4 $\sim$ 2.1)[7]. The value of the proportion of rash symptoms θ is 98.3% according to the technical reports of US CDC[8]. In our estimation process, the baseline forgetting factor λ is 0.65. As for the date range of COVID-19, the start date is listed in Appendix C and we simulate the same time length as the mpox simulation in four countries.

4.2. Simulation results and analysis

In this section, we first review the mpox situation in those four countries in Appendix D, providing basic information about the outbreak. Then we utilize the vSEIR model, using the available data, to perform the simulation of the mpox epidemic which is shown in Fig. 2 and give the number of the actively infected people that cannot be observed in daily reports. The simulation result of COVID-19 is listed in Fig. C.7 in Appendix C. The metrics we use in evaluating our model are root mean square deviation (RMSE) and coefficient of determination (R^2), that is

$$RMSE = \frac{\sqrt{\sum_{t=0}^{T}\left(C(t)-\hat{C}(t)\right)^2}}{T+1},$$

and

$$R^2 = 1-\frac{\sum_{t=0}^{T}\left(\hat{C}(t)-C(t)\right)^2}{\sum_{t=0}^{T}\left(\overline{C}(t)-C(t)\right)^2},$$

where t denotes the simulation date, T denotes the number of days being simulated, $C(t)$ denotes actual cumulative reported cases, $\hat{C}(t)$ denotes the simulated cumulative reported cases and $\bar{C}(t) = (\sum_{t=0}^{T} C(t))/(T+1)$. The evaluation result is in Table 2 (The experiment of the other two alternative forgetting factors are also listed in Table E.5 in Appendix E). The relatively small RMSE and that R^2 is extremely close to 1 indicate that our model is of high accuracy.

[7] `https://www.who.int/news-room/fact-sheets/detail/monkeypox` (retrieved on 28th February 2023)

[8] `https://www.cdc.gov/poxvirus/mpox/response/2022/index.html` (retrieved on 28th February 2023)

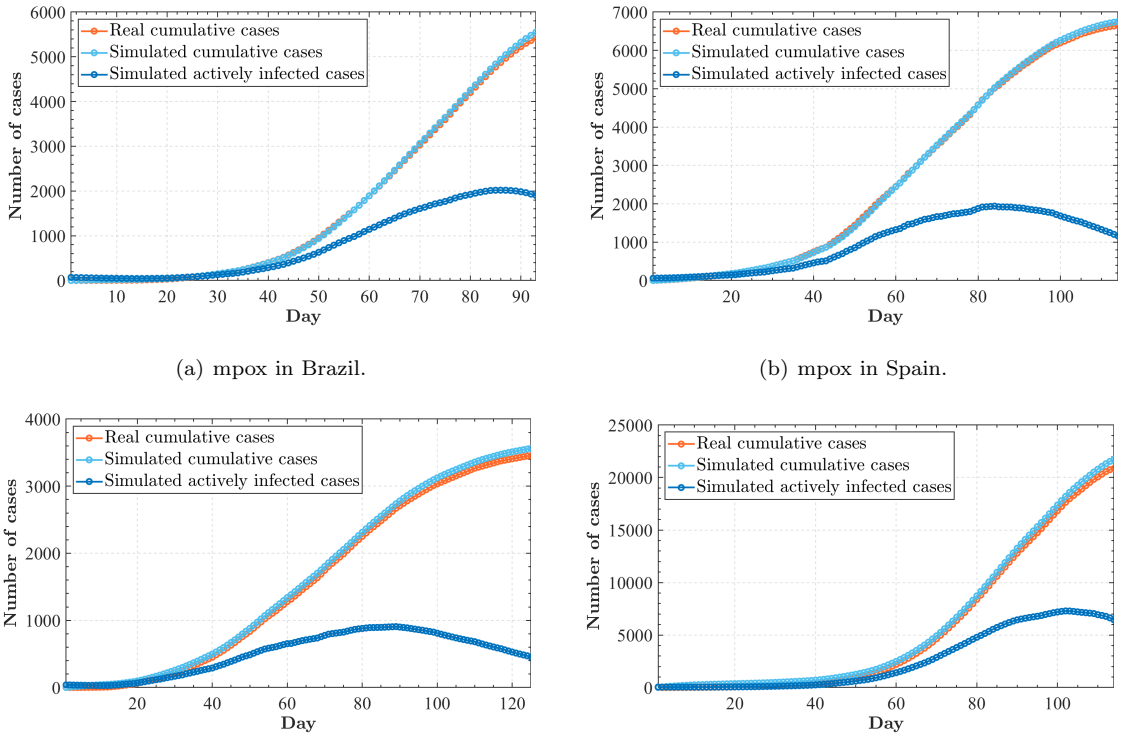

(a) mpox in Brazil.

(b) mpox in Spain.

(c) mpox in UK.

(d) mpox in US.

Figure 2: The simulation results of four countries.

Table 2: The evaluation results of the four countries being estimated

Country	Brazil	Spain	UK	US
RMSE	33.9000	43.7261	80.4324	48.1615
R^2	0.9998	0.9997	0.9966	0.9900

According to the value of the cumulative reported cases as the orange line that can be obtained directly, the value can be interpreted with the review and report from Appendix D, then according to the simulated actively infected data that cannot be observed from the daily report, we can get the actual situation that the active infected people experienced declines between approximately day 80 and day 110 of the mpox outbreak in these four countries.

In fact, we additionally conduct a simulation on the trend of mpox infection in four countries in October and November, as depicted in Fig. F.9 in Appendix F, which shows a stable but low rate of emergence of new cases. This is consistent with the end of the experiment period. To effectively prevent the resurgence of mpox epidemic, it is essential to maintain vigilance.

4.3. Effective reproduction number filtration and analysis

In this section, we calculate the R_t of the four countries based on Eq. (2). Moreover, we use the sparse HP filter to produce the piecewise value of R_t and capture the kinks based on that value, which is shown in

Fig. 3. The grey line is the estimated R_t based on the vSEIR model, the blue dashed line is the filtered value of R_t via sparse HP filter and the red vertical line denotes the kinks. Eventually, the periods of mpox and COVID-19 in four countries are calculated based on the kinks. Furthermore, by using a filtered R_t, we can draw more accurate conclusions about the properties of these epidemics. It is not appropriate to compare the situations of mpox and COVID-19 based on the breaks or sharp turns in the estimated R_t. Instead, a filtered value of R_t allows for a more reasonable and feasible analysis of epidemic properties and can help us interpret the estimated kinks and define the periods of mpox and COVID-19 in these four countries. This, in turn, enables us to make more meaningful comparisons between mpox and COVID-19 in terms of their kink properties.

Since the actively infected people are on the decline according to our simulation results, we deduce that there will be at least 1 kink in each country. Moreover, we believe that during the outbreak period, the kinks will not be a large number and if the amount of kinks is too large, it will be difficult to explain these kinks. Apart from that, because μ is a relatively large number [23], we choose a fairly wide possible set. Therefore, in the selection of tuning parameters, we set the possible values of χ belongs to $X = \{1, 2, 3, 4\}$ and μ belongs to $U = \{1, 10, 100, 1000, 10000\}$. In this process, we choose the tune parameters of $(\chi, \mu) = (4, 1)$ to perform the best kink estimation result based on the selection of tuning parameters via criterion (13), which is shown in Figs. 3 and 4.

The selection result of COVID-19 is shown in Fig. C.8 in Appendix C. We look at Brazil and US as benchmark countries and provide analysis and comparison.

4.3.1. Brazil

COVID-19 was confirmed to have spread to Brazil on February 20, 2020, and the first case of mpox was reported on June 8, 2022. This has shown similar results to those seen in US, and it appears that the mpox cases will continue for a period of time, as its R_t has been above 1 for most of the time. Therefore, it is important for the government to introduce measures to ensure that mpox does not spread too far. The estimated kink dates are Day 11 (June 19), Day 21 (June 29), Day 31 (July 09), and Day 33 (July 11), which corresponded to five periods of mpox in Brazil.

Period 1: Day 0 $\sim$ 11 (June 09 $\sim$ June 19): This period corresponded to the initial epidemic wave.

Period 2: Day 11 $\sim$21 (June 19 $\sim$ June 29): The R_t experienced a sharp growth and reaches its peak.

Period 3: Day 21 $\sim$ 31 (June 29 $\sim$ July 09): The R_t experienced a sharp decline.

Period 4: Day 31 $\sim$ 33 (July 09 $\sim$ July 11): The R_t growed from the previous decline as the second wave.

Period 5: Day 33 $\sim$ 88 (July 11 $\sim$ September 25): The R_t decreased but less steeply, finally below 1.

Brazil's mpox epidemic has three periods of increase and two periods of decrease, which is different from the pattern seen in Brazil's COVID-19 epidemic. As shown in the first two subplots of Fig. 3, mpox reaches its last period on Day 33 (July 11), which is one day earlier than the last period in the Brazil COVID-19 epidemic. This delay is not as significant as the result seen in US, which suggests that mpox may pose

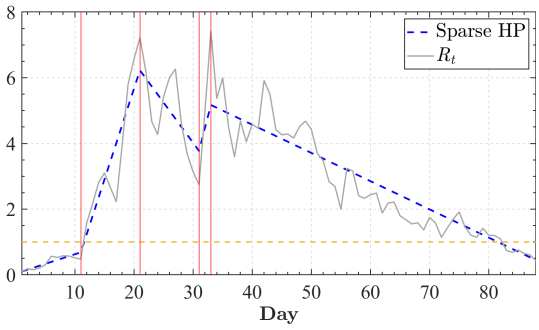

(a) mpox in Brazil.

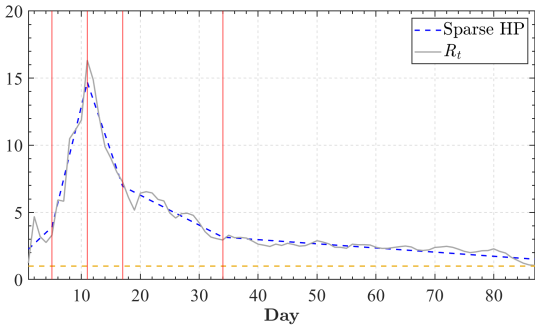

(b) COVID-19 in Brazil.

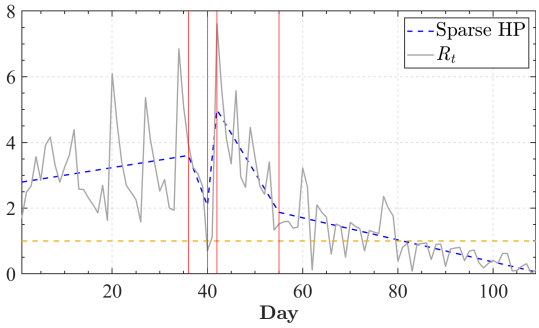

(c) mpox in Spain.

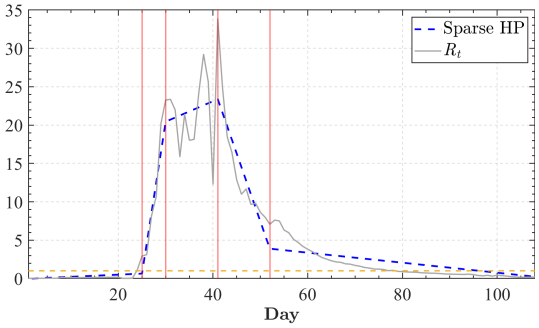

(d) COVID-19 in Spain.

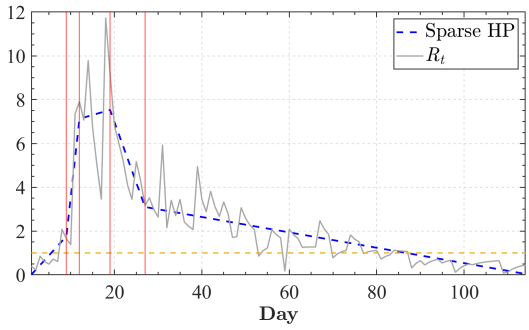

(e) mpox in UK.

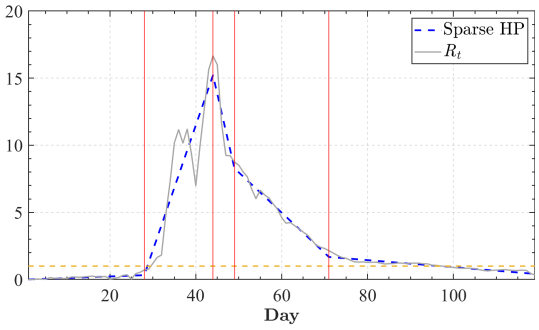

(f) COVID-19 in UK.

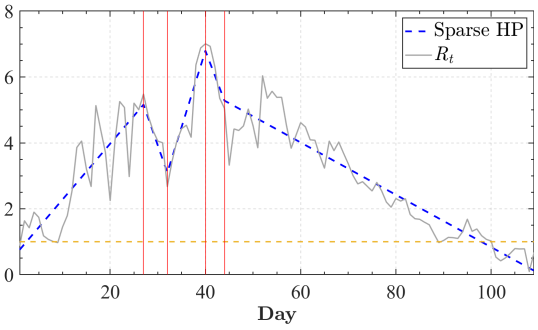

(g) mpox in US

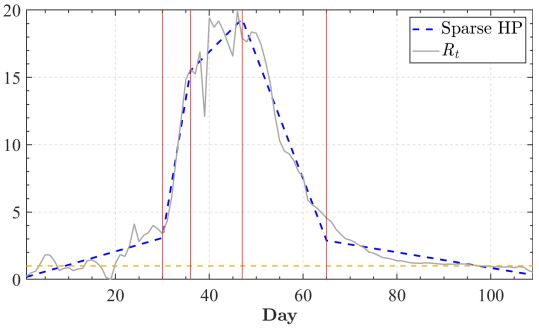

(h) COVID-19 in US.

Figure 3: mpox and COVID-19 in four countries via sparse HP filter.

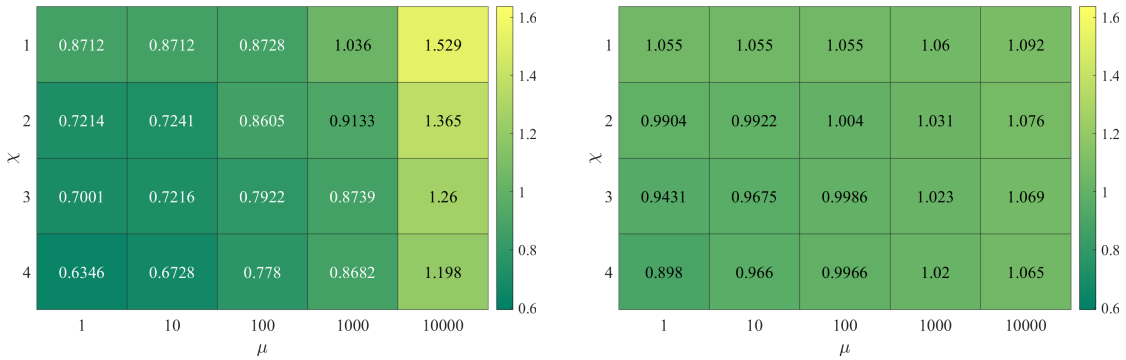

(a) mpox in Brazil.

(b) mpox in Spain.

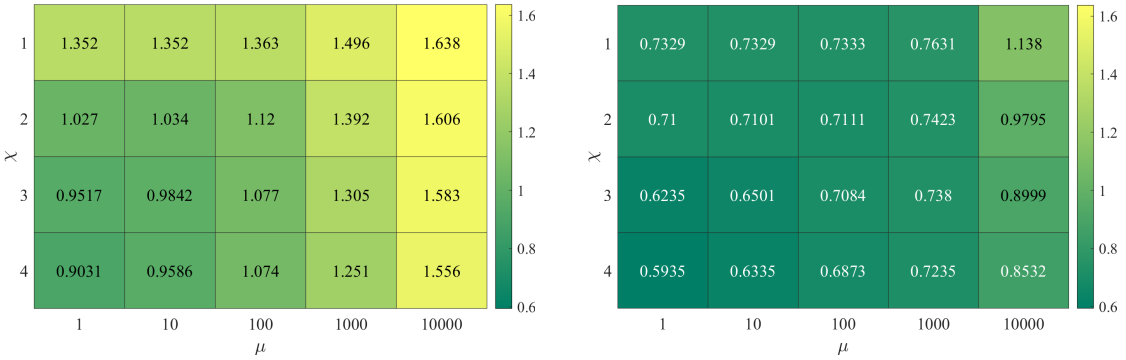

(c) mpox in UK.

(d) mpox in US.

Figure 4: Selection of tuning parameters in four countries. The number in the figure represents the value of the objective function (13).

some future problems in Brazil. It is worth noting that the decrease in R_t is the result of social distancing measures, which may indicate that the government needs to issue laws similar to its COVID-19 control policies to prevent the potential spread of mpox. Furthermore, the decrease period in Brazil's COVID-19 epidemic occurs immediately after the increase period, which suggests that the decrease period is the result of strong interventions. In contrast, the decrease period of Brazil's mpox epidemic occurs between the three waves of increase, which may indicate some restrictions on its spreadability based on the properties of mpox infection. Therefore, it is necessary for the government to prepare some restriction strategies to prevent the resurgence of mpox infections.

4.3.2. US

The start date of COVID-19 was January 22, 2020, and the start date of mpox was May 18, 2022. According to the results of the vSIADR model [5], the R_t of COVID-19 at the beginning of April was around 5, which is similar to our result on Day 74 (April 04). On July 28, US Centers for Disease Control and Prevention (CDC) released the first issue of the technical report on mpox, which may help the public better understand how to prevent mpox. Through these public awareness campaigns, the R_t of mpox began to decline and eventually fell below 1. The decrease in R_t for COVID-19, on the other hand, is likely the result

of strong interventions such as isolation policies and the widespread use of face masks. The estimated kink dates are Day 27 (July 13), Day 32 (July 18), Day 40 (July 26), and Day 44 (July 30), which corresponded to five periods of mpox in US.

Period 1: Day 0 $\sim$ 27 (May 17 $\sim$ July 13): This period corresponded to the initial epidemic wave.

Period 2: Day 27 $\sim$ 32 (July 13 $\sim$ July 18): This period corresponded to the short break from the growth of R_t.

Period 3: Day 32 $\sim$ 40 (July 18 $\sim$July 26): The R_t peaked at the end of this period as the second wave.

Period 4: Day 40 $\sim$ 44 (July 26 $\sim$ July 30): The R_t experienced a sharp decrease.

Period 5: Day 44 $\sim$ 109 (July 30 $\sim$ September 25): The R_t decreased but less steeply, finally below 1.

The mpox epidemic in US has two periods of increase and three periods of decrease, which is the same pattern as seen in US COVID-19 epidemic. As shown in the two subfigures in Fig. 3, mpox reaches its last period on Day 44 (July 30), which is 21 days earlier than the last period in US COVID-19 epidemic. It is worth noting that the decrease in R_t is mainly due to public awareness campaigns on social distancing, rather than mandatory measures. This suggests that the mpox epidemic reached its decline stage without the need for strong interventions. In contrast, the decrease period in US COVID-19 epidemic occurs immediately after the increase period, which suggests that the decrease is the result of strong interventions. In comparison, the decrease period of US mpox occurs between the two waves of increase, which leads to similar results as seen in Brazil.

4.3.3. UK

The start date of COVID-19 was January 22, 2020, and the start date of mpox was May 06, 2022. The spread of mpox was characterized by a rapid surge in cases, with the number of cases doubling every week. Nevertheless, in response to UK's Health Security Agency's first technical report, issued on June 21, which indicated that the mpox virus was highly homologous and showed no sign of spreading, as well as the introduction of protective measures, the R_t of mpox showed a steady decline below 1. In comparison to COVID-19 in UK, the virus was also controlled through measures such as working from home and medical treatment, which were not seen in the treatment of mpox. The estimated kink dates are Day 9 (May 15), Day 12 (May 18), Day 19 (May 25), and Day 24 (May 30), which corresponds to five periods of mpox in UK.

Period 1: Day 0 $\sim$ 9 (May 06 $\sim$ May 15): This period corresponded to the initial epidemic wave.

Period 2: Day 9 $\sim$ 12 (May 15 $\sim$ May 18): The R_t experienced a sharp increase in a short period.

Period 3: Day 12 $\sim$ 19 (May 18 $\sim$ May 25): The R_t experienced a slowed increase and reaches the peak.

Period 4: Day 19 $\sim$ 24 (May 25 $\sim$ May 30): The R_t started to decline at a fast speed.

Period 5: Day 24 $\sim$ 113 (May 30 $\sim$ September 25): The R_t decreased but less steeply, finally below 1.

4.3.4. Spain

The start date of COVID-19 was January 22, 2020, and the start date of mpox was May 18, 2022. Similar to the situation in UK, mpox distributes a mild increase above 1 followed by a decline. This may be due to

the fact that mpox is self-limiting and the number of infected individuals is relatively small, which requires close contact for transmission. The estimated kink dates are Day 36 (June 23), Day 40 (June 27), Day 42 (June 29), and Day 55 (July 12), which corresponds to five periods of mpox in Spain.

Period 1: Day 0 $\sim$ 36 (May 18 $\sim$ June 23): This period corresponded to the initial epidemic wave.

Period 2: Day 36$\sim$ 40 (June 23 $\sim$ June 27): The R_t experienced a sharp decline in a short period.

Period 3: Day 40 $\sim$ 42 (June 27 $\sim$ June 29): The R_t experienced a sharp increase and reaches the peak.

Period 4: Day 42 $\sim$ 55 (June 29 $\sim$ July 12): The R_t started to decline at a fast speed.

Period 5: Day 55 $\sim$ 109 (July 12 $\sim$ September 25): The R_t decreased but less steeply, finally below 1.

All in all, UK has a relatively early period of reaching their last period while Spain has a similar date of last period in its COVID-19 and mpox epidemic. However, the total infections in Spain is relatively small, which is not as serious as its COVID-19 epidemic. Overall, we see that the last period of mpox is ahead of that in COVID-19 except for Spain, which means that mpox may reach its decline period earlier than COVID-19 and the value of R_t is usually lower than that of COVID-19. However, it is worth noting that the situation in Brazil has the closest date of the last period in mpox and COVID-19. Therefore, we conclude that even though mpox has a weaker infection ability compared with COVID-19, prevention strategies should still be implemented to prevent its resurgence, especially in Brazil, where there have been three periods of increase.

5. Sensitivity analysis for mpox modelling

In this section, we mainly conduct two analysis procedures, the first is the analysis regarding the situation without smallpox vaccine protection in Section 5.1, followed by the uncertainty analysis for the lag in reported cases of mpox in Section 5.2. Through those two analyses, more insights will be put into mpox spreading.

5.1. Situation without smallpox vaccine protection

In the proposed scenario, we envision a situation devoid of smallpox vaccine protection. In particular, we modify the parameter τ in model (1), altering its value from 0.15 to 1. We then implement the simulation model across four countries to compute the variations in the total number of infection cases. The results delineated in the corresponding Table 3 indicate that in the absence of smallpox vaccine protection, there is a projected increase in the total infection cases by approximately 12% for each country under study. Therefore, as a short-term measure, the government can take the approach of vaccinating high-risk individuals against smallpox to control the potential resurgence of mpox epidemic.

Table 3: The change of infections in the absence of smallpox vaccine protection

Country	Default	Without protection	Increase
Brazil	6,775	7,651	12.9%
Spain	6,815	7,766	13.9%
UK	3,550	3,999	12.6%
US	21,519	24,157	12.3%

5.2. Uncertainty in reported cases

We also consider a situation accounting for the uncertainty in the reporting and reporting delay of mpox cases due to the quality of the report data[9] [26], which we call the test latency. Test latency analysis is essential because the delay between the time of infection and the time of report can greatly impact our simulation results [27]. Test latency analysis is also crucial for policy making. Policymakers should carefully consider the results of test latency analysis because simulation models based on reported data may not be completely accurate. For example, even if the model simulation results show that the effective reproduction number is lower than 1 at the end of the outbreak, the test latency analysis results may show a large difference in the outcome. This is reasonable because the number of reported cases may not accurately reflect the true situation due to various factors. Therefore, experts must ensure that the test latency results are also consistent with the policy measures being implemented to control mpox.

Thanks to the symptoms of mpox being more obvious than COVID-19, the report of the cases may be much easier than COVID-19 cases, and we may choose some relatively small numbers in defining the lag between the test and report. In particular, we assume that the observed number of daily infections $C(t)$ follows Poisson distribution, which is widely done in other works in estimating the daily infection [5, 26], that is, we use the real daily increment $\widetilde{C}(t)$ instead of reported daily cases $C(t)$ with $\widetilde{C}(t) \sim \text{Poisson}(C(t+\Delta t))$. We conduct two simulation analyses: $\Delta t = 1$ and $\Delta t = 3$, i.e., we consider a lag of 1 or 3 days between the infection and reporting and, on each day, the expectation of the number of observed infections is the number of infections 1 or 3 days before.

We then proceed with generating two Monte Carlo samples [28] of size $10,000$, for the daily infections $\widetilde{C}(t)$, and run the vSEIR model and get the upper and lower limit of the estimated R_t in four countries, the whole process can be explained into Algorithm 2 in Appendix G. The entire analysis takes about twenty minutes per sample. Fig. 5 shows the results of Brazil, Spain, UK, US. The deep blue line is the original estimated R_t. Note that most of the estimated data fall in the 95% prediction interval, but by the end of the outbreak period as well as at some certain time, the original R_t falls out from the interval, which shows the necessity of the uncertainty in reported cases analysis. Through our analysis, we have identified some concerns: in some countries, such as UK and Brazil, the upper bound of R_t is still above 1 at the end of the

[9] `https://www.who.int/news/item/11-05-2023-fifth-meeting-of-the-international-health-regulations-(2005)-(ihr)-emergency-committee-on-the-multi-country-outbreak-of-monkeypox-(mpox)` (retrieved on 25th May 2023)

experiment period, which may indicate that mpox still requires measures to prevent its potential resurgence.

Besides, in relation to the uncertainty regarding incubation and recovery rate, the analysis conducted in Appendix H indicates that in the majority of countries, the 95% confidence interval does not exceed 10. However, when examining the upper confidence interval for the test latency analysis in section 5.2, it surpasses 10, and in some cases even 15, with the exception of the United States. This finding suggests that the existing data reporting process may not be effective enough to accurately portray the real mpox situation. Consequently, in order to effectively prevent any future resurgence of mpox,it is imperative to improve the mpox data quality and report process.

6. Discussion and conclusions

In this paper, we develop a novel setup named the vSEIR model, an extended version of the traditional SEIR model accounting for seniors potentially protected by smallpox vaccines and time-varying infectious rate, to better simulate the early mpox outbreak. The FRLS algorithm is successfully applied to the online estimation of time-varying infection rate in the discrete vSEIR model to reflect the intervention level concerning the transmission of the mpox virus. In addition to the consideration of the mpox epidemic, we comparatively analyze the effective reproduction number R_t of the COVID-19 and mpox in their early outbreak period, and the corresponding results display that the R_t of COVID-19 is much higher than that of mpox, which means that the transmission ability of mpox is worse than COVID-19. Moreover, we introduce the sparse HP filter to produce piecewise estimations of R_t. After that, the development periods of the mpox epidemic in Brazil, Spain, US, and UK are given based on those kinks. We then find that the date of the declining period of mpox is earlier than COVID-19, which means that mpox may be easier to control.

To further explore the potential situation of the mpox epidemic, we first consider the situation without the smallpox protection, next we use the Monte Carlo method to conduct the uncertainty analysis regarding the impact of the possible lag in reported data. We surprisingly find that the second situation brings R_t wider confidence intervals, consequently, we sincerely recommend that the government make every effort to optimize the reporting mechanism of epidemic data, providing enough reliable data to give a true picture of the development of the mpox epidemic.

This work can be extended to include vaccination strategies that are developed after the outbreak, which would allow for a more detailed accounting of the decreasing population of susceptible individuals in some cases. Additionally, the current model uses a fixed vaccine failure rate in the aged susceptible compartment. Improving on this, the model could use varied values from medical data in the vaccine failure rate for greater accuracy. Adjusting these two factors would result in a longer-term and better results.

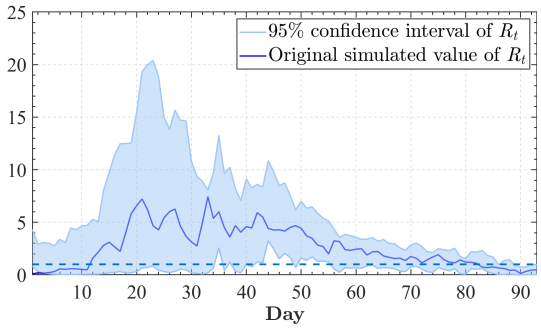

(a) Test latency result of 1-day delay in Brazil

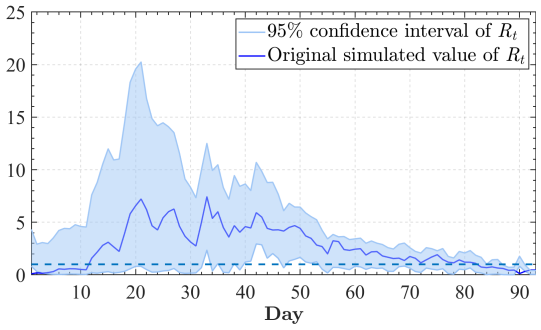

(b) Test latency result of 3-day delay in Brazil

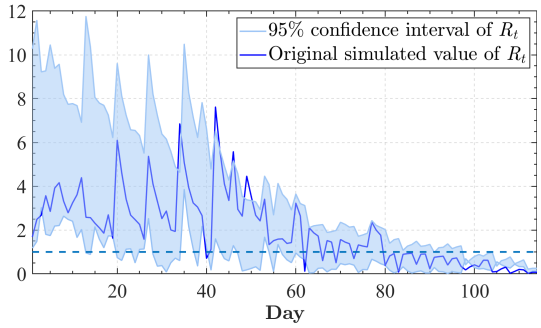

(c) Test latency result of 1-day delay in Spain

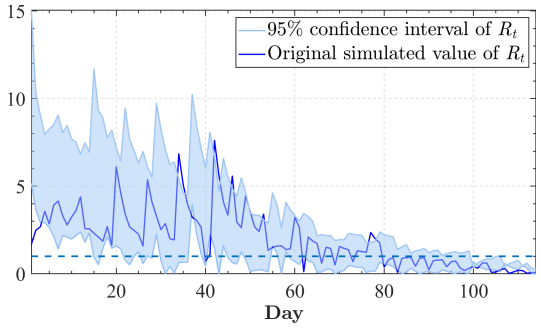

(d) Test latency result of 3-day delay in Spain

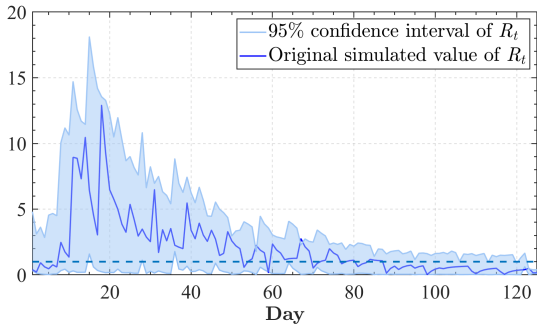

(e) Test latency result of 1-day delay in UK

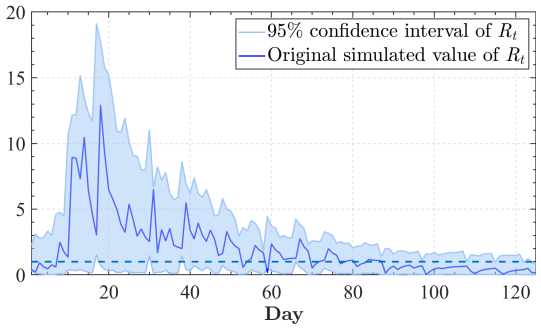

(f) Test latency result of 3-day delay in UK

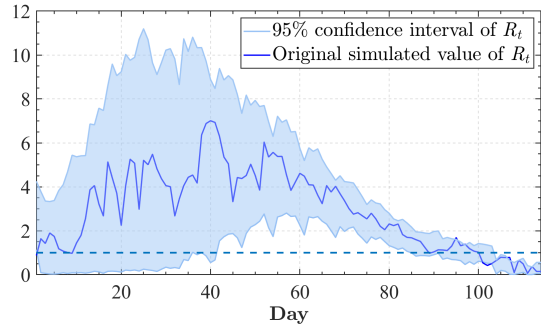

(g) Test latency result of 1-day delay in US

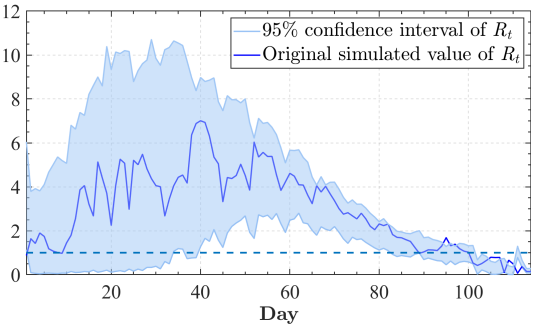

(h) Test latency result of 3-day delay in US

Figure 5: Test latency result of 1-day and 3-day lag of mpox in four countries.

Acknowledgement

This paper is supported by the National Natural Science Foundation of China (Grant No. 71872110). The authors would like to thank the anonymous reviewers and editors' useful comments to make this paper more comprehensive. The authors would also like to thank Xinhao Sun, Jiheng Tan and Jie Fang for their support of our paper.

References

[1] A. Zumla, S. R. Valdoleiros, N. Haider, D. Asogun, Monkeypox outbreaks outside endemic regions: scientific and social priorities, The Lancet Infectious Diseases 22 (7) (2022) 929–931. doi:10.1016/S1473-3099(22)00354-1.

[2] A. Sharma, Priyanka, M. Loganathan, O. P. Choudhary, Monkeypox outbreak: New zoonotic alert after the covid-19 pandemic, International Journal of Surgery 104 (2022) 106812. doi:https://doi.org/10.1016/j.ijsu.2022.106812.

[3] M. Marietta, V. Coluccio, M. Luppi, Monkeypox outbreak: After COVID-19, another challenge for the hemostatic system?, Internal and Emergency Medicine 17 (8) (2022) 2179–2183. doi:10.1007/s11739-022-03112-8.

[4] A. G. Mukherjee, U. R. Wanjari, S. Kannampuzha, S. Das, R. Murali, et al., The pathophysiological and immunological background of the monkeypox virus infection: An update, Journal of Medical Virology 95 (1) (2023) e28206. doi:https://doi.org/10.1002/jmv.28206.

[5] H. Yan, Y. Zhu, J. Gu, Y. Huang, H. Sun, X. Zhang, et al., Better strategies for containing COVID-19 pandemic: A study of 25 countries via a vSIADR model, Proceedings of the Royal Society A 477 (2248) (2021) 20200440. doi:10.1098/rspa.2020.0440.

[6] J. Song, H. Xie, B. G. et al., Maximum likelihood-based extended Kalman filter for COVID-19 prediction, Chaos, Solitons & Fractals 146 (2021) 110922. doi:10.1016/j.chaos.2021.110922.

[7] J. Cai, J. Zhou, How many asymptomatic cases were unconfirmed in the US COVID-19 pandemic? The evidence from a serological survey, Chaos, Solitons & Fractals 164 (2022) 112630. doi:10.1016/j.chaos.2022.112630.

[8] R. Grant, L.-B. L. Nguyen, R. Breban, Modelling human-to-human transmission of monkeypox, Bulletin of the World Health Organization 98 (9) (2020) 638. doi:10.2471/BLT.19.242347.

[9] L. Zhang, J. Huang, B. Chen, Y. Zhao, D. Wang, W. Yan, Global prediction for monkeypox epidemic (2020), medRxiv. doi:10.1101/2022.10.21.22280978.

[10] O. J. Peter, F. A. Oguntolu, et al., Fractional order mathematical model of monkeypox transmission dynamics, Physica Scripta 97 (8) (2022) 084005. doi:10.1088/1402-4896/ac7ebc.

[11] O. J. Peter, S. Kumar, N. Kumari, F. A. Oguntolu, K. Oshinubi, R. Musa, Transmission dynamics of Monkeypox virus: A mathematical modelling approach, Modeling Earth Systems and Environment (8) (2021) 3423–3434. doi:10.1007/s40808-021-01313-2.

[12] J. Chadha, L. Khullar, P. Gulati, S. Chhibber, K. Harjai, Insights into the monkeypox virus: Making of another pandemic within the pandemic?, Environmental Microbiology 24 (10) (2022) 4547–4560. doi:10.1111/1462-2920.16174.

[13] Z. Kang, H. He, J. Liu, X. Ma, M. Gui, Adaptive pulsar time delay estimation using wavelet-based RLS, Optik 171 (2018) 266–276. doi:10.1016/j.ijleo.2018.05.118.

[14] R. Grant, L. B. L. Nguyen, R. Breban, Modelling human-to-human transmission of monkeypox, Bulletin of the World Health Organization 98 (2020) 638–640. doi:10.2471/BLT.19.242347.

[15] S. W. X. Ong, T. Chia, B. E. Young, SARS-CoV-2 variants of concern and vaccine escape, from Alpha to Omicron and beyond, Expert Review of Respiratory Medicine 16 (5) (2022) 499–502. doi:10.1080/17476348.2022.2057299.

[16] Akter, Fahima and Hasan, Tahira Binte and Alam, et al., Effect of prior immunisation with smallpox vaccine for protection against human monkeypox: A systematic review (2023) e2444. doi:10.1002/rmv.2444.

[17] P. van den Driessche, Reproduction numbers of infectious disease models, Infectious Disease Modelling 2 (2017) 288–303. doi:10.1016/j.idm.2017.06.002.

[18] R. Merched, A. Sayed, Order-recursive RLS Laguerre adaptive filtering, IEEE Transactions on Signal Processing 48 (11) (2000) 3000–3010. doi:10.1109/78.875457.

[19] A. P. Costa, J. S. Møller, H. K. Iversen, S. Puthusserypady, An adaptive CSP filter to investigate user independence in a 3-class MI-BCI paradigm, Computers in Biology and Medicine 103 (2018) 24–33. doi:10.1016/j.compbiomed.2018.09.021.

[20] M. Angeli, G. Neofotistos, M. Mattheakis, E. Kaxiras, Modeling the effect of the vaccination campaign on the COVID-19 pandemic, Chaos, Solitons & Fractals 154 (2022) 111621. doi:https://doi.org/10.1016/j.chaos.2021.111621.

[21] Z. Liao, P. Lan, X. Fan, B. Kelly, A. Innes, Z. Liao, SIRVD-DL: A COVID-19 deep learning prediction model based on time-dependent SIRVD, Computers in Biology and Medicine 138 (2021) 104868. doi:https://doi.org/10.1016/j.compbiomed.2021.104868.

[22] A. Di Crescenzo, P. Paraggio, P. Román-Román, F. Torres-Ruiz, Applications of the multi-sigmoidal deterministic and stochastic logistic models for plant dynamics, Applied Mathematical Modelling 92 (2021) 884–904. doi:10.1016/j.apm.2020.11.046.

[23] S. Lee, Y. Liao, M. H. Seo, Y. Shin, Sparse HP filter: Finding kinks in the COVID-19 contact rate, Journal of Econometrics 220 (1) (2021) 158–180. doi:10.1016/j.jeconom.2020.08.008.

[24] Remigijus Paulavičius, Julius Žilinskas, Andreas Grothey, Investigation of selection strategies in branch and bound algorithm with simplicial partitions and combination of Lipschitz bounds, Optimization Letters 4 (2010) 173–183. doi:10.1007/s11590-009-0156-3.

[25] M. U. G. Kraemer, H. Tegally, D. M. Pigott, A. Dasgupta, J. Sheldon, Tracking the 2022 monkeypox outbreak with epidemiological data in real-time, The Lancet Infectious Diseases 22 (7) (2022) 941–942. doi:10.1016/S1473-3099(22)00359-0.

[26] S. Han, J. Cai, J. Yang, J. Zhang, Q. Wu, W. Zheng, et al., Time-varying optimization of COVID-19 vaccine prioritization in the context of limited vaccination capacity, Nature Communications 12 (1) (2021) 1–10. doi:10.1038/s41467-021-24872-5.

[27] M. Shoaib, A. Haider, M. A. Z. Raja, K. S. Nisar, Artificial intelligence knacks-based computing for stochastic COVID-19 SIRC epidemic model with time delay, International Journal of Modern Physics B 36 (26) (2022) 2250174. doi:10.1142/S0217979222501740.

[28] I. Buvat, D. Lazaro, Monte Carlo simulations in emission tomography and GATE: An overview, Nuclear Instruments and Methods in Physics Research Section A: Accelerators, Spectrometers, Detectors and Associated Equipment 569 (2) (2006) 323–329. doi:10.1016/j.nima.2006.08.039.

[29] E. Dong, H. Du, L. Gardner, An interactive web-based dashboard to track COVID-19 in real time, The Lancet Infectious Diseases 20 (5) (2020) 533–534. doi:10.1016/S1473-3099(20)30120-1.

[30] X. Lu, E. Borgonovo, Global sensitivity analysis in epidemiological modeling, European Journal of Operational Research 304 (1) (2023) 9–24. doi:10.1016/j.ejor.2021.11.018.

[31] F. Miura, C. E. van Ewijk, J. A. Backer, M. Xiridou, E. Franz, de Coul, Estimated incubation period for monkeypox cases confirmed in the Netherlands, May 2022, Eurosurveillance 27 (24) (2022) 2200448. doi:10.2807/1560-7917.ES.2022.27.24.2200448.